Molecular Vision 2023; 29:329-337 <http://www.molvis.org/molvis/v29/329>
Received 11 April 2023 | Accepted 10 December 2023 | Published 15 December 2023

Novel pathogenic variants in Tubulin Tyrosine Like 5 (*TTLL5)* associated with cone-dominant retinal dystrophies and an abnormal optical coherence tomography phenotype

Olubayo U. Kolawole, Cheryl Y. Gregory-Evans, Riyaz Bikoo, Albert Z. Huang, Kevin Gregory-Evans

Department of Ophthalmology and Visual Sciences, University of British Columbia, Canada

Purpose: Autosomal recessive cone and cone-rod dystrophies (CD/CRD) are inherited forms of vison loss. Here, we report on and correlate the clinical phenotypes with the underlying genetic mutations.
Methods: Clinical information was collected from subjects, including a family history with a chart review. They underwent a full ophthalmic examination, including best-corrected visual acuity, direct and indirect ophthalmoscopy, color vision testing, color fundus photography, contrast sensitivity, autofluorescence, and spectral domain–optical coherence tomography (SD–OCT), and full-field electroretinography. Next-generation panel-based genetic testing was used to identify DNA variants in subject buccal swab samples.
Results: Genetic testing in two patients revealed three novel variants in the *TTLL5* gene associated with CD/CRD: two missense variants (c.1433G>A;p.(Arg478Gln), c.241C>G;p.(Leu81Val), and one loss-of-function variant (c.2384_2387del;p.(Ala795Valfs*9). Based on *in-silico* analysis, structural modeling, and comparison to previously reported mutations, these novel variants are very likely to be disease-causing mutations. Combining retinal imaging with SD-OCT analysis, we observed an unusual sheen in the CD/CRD phenotypes.
Conclusion: Based on the protein domain location of novel *TTLL5* variants and the localization of TTLL5 to the connecting cilium, we conclude that the CD/CRD disease phenotype is characterized as a ciliopathy caused by protein tracking dysfunction. This initially affects cone photoreceptors, where photoreceptor cilia express a high level of TTLL5, but extends to rod photoreceptors over time. Fundus photography correlated with SD-OCT imaging suggests that the macular sheen characteristically seen with *TTLL5* mutations derives from the photoreceptor's outer segments at the posterior pole.

Cone and cone-rod dystrophies (CD/CRD) are a group of rare inherited retinal degenerations that are phenotypically and genetically heterogeneous [1]. Visual impairment is primarily due to the loss of cone photoreceptors causing a loss of visual acuity, abnormal color vision, photophobia, and central scotomas. Some forms of CD/CRD are progressive, leading to a loss of peripheral vision [2]. Mutations in 37 genes have been linked to CD/CRD (https://sph.uth.edu/retnet/sum-dis.htm#B-diseases, accessed 10 Mar 2023); however, more than 30% of simplex/recessive cases remain to be solved [3].

One of the more recently identified genes causing CD is *TTLL5*, which codes for the tubulin tyrosine ligase-like family member 5 protein [4]. Initially, mutations in the *TTLL5* gene were found in four families with CD [5]; however, more recently, *TTLL5* mutations have been associated with other phenotypes, including CRD, sectoral CRD, and early-onset severe retinal dystrophy [6–11].

Correspondence to: Kevin Gregory-Evans, Department of Ophthalmology and Visual Sciences University of British Columbia 2550 Willow Street Vancouver, BC V5Z 3N9, Canada; Phone: 1-604-671-0419; FAX: 1-604-675-3010; email: kge30@mail.ubc.ca

TTLL5 glutamylase catalyzes posttranslational modifications of α-tubulin in the axonemes of cilia [12]. Recently, it was shown that TTLL5 glutamylates both glutamate and glycine amino acids in the $RPGR^{ORF15}$ protein, which localizes to the connecting cilia of photoreceptor cells [13]. In *Ttll5* knockout mice, $RPGR^{ORF15}$ is not glutamylated, resulting in opsin mislocalization and photoreceptor degeneration [14]. Thus, *TTLL5*-associated retinal dystrophy is a ciliopathy due to $RPGR^{ORF15}$ protein tracking dysfunction. Cone photoreceptor cilia express a higher level of TTLL5 protein compared to rods [5], which may explain why cones are affected first in this group of diseases. Here, we report 3 novel *TTLL5* mutations in two families with CD/CRD and describe a novel feature observed by spectral domain optical coherence tomography (SD-OCT) that may explain the retinal sheen observed in this phenotype.

METHODS

Study subjects: This study was approved by the clinical research ethics board of the University of British Columbia and adhered to the tenets of the Declaration of Helsinki. Three subjects were examined by retina specialists at the Eye Care Centre in Vancouver, Canada. The data presented are based

on a retrospective chart review, with diagnoses established from clinical assessment and supported by genetic testing results. Informed consent was obtained from all subjects included in the study.

Clinical assessment: For each study subject, a family history was taken to establish the likely inheritance pattern. All subjects had Caucasian ethnicity. An ophthalmic examination included best-corrected visual acuity, direct and indirect ophthalmoscopy, and slit-lamp biomicroscopy. In addition, the examination included color vision testing, color fundus photography (wide-field camera; Optos, Inc., Marlborough, MA, or Topcon narrow-field fundus camera, Oakland, NJ), contrast sensitivity, autofluorescence, and spectral domain optical coherence tomography (SD-OCT). Measurements of retina thickness and the size of the ellipsoid zone were made using OCT software. Full-field electroretinography (ffERG), according to the International Society for Clinical Electrophysiology of Vision (ISCEV) standards, was available for one subject.

Molecular genetic testing: Buccal swabs were taken for DNA testing and screened using a panel of 351 genes associated with retinal dystrophy (Blueprint Genetics, Marlborough, MA). This panel included the maternally inherited mitochondrial genome and well-established non-coding variants. Evaluations of the variants identified and interpretations were based on criteria established by the American College of Medical Genetics and Genomics [15]. The results were correlated with the subject's clinical diagnosis and family history, and each subject received genetic counseling for their test results.

Structural modeling: 3D protein: We used the freely available missence3d package to predict the structural changes introduced into a protein by amino acid substitution [16]. The UniProt ID for the 1,281-amino-acid protein TTLL5 is Q6EMB2. We accessed the AlphaFold predicted structure platform [17], found the alpha helix for TTLL5, and then downloaded the protein data bank (PDB) file of the structure. The Arg478 residue maps with high confidence to the alpha helix structure which would suggest that changes at this residue would disrupt the protein function. The PDB file was uploaded to the missence3d software along with the specific amino acid substitution.

RESULTS

Clinical assessment: Female subject 1 (P1) presented in 2013 at age 43 with vision loss for 3 years and a history of high myopia (−12.00D right and −8.00D left), dyschromatopsia, central visual field loss, and decreased central vision. Best-corrected visual acuity (BCVA) was 20/40 right and 20/30 left, and photosensitivity to light. Dilated fundus examination (Figure 1A,B) revealed myopic crescents, abnormal pigmentation in the foveal region, and a central mild macular sheen. In the peripheral retina, there were extensive white beads reminiscent of Pearl degeneration. SD-OCT (Figure 1C) revealed central macular atrophy with the disruption of the ellipsoid zone and outer nuclear layer thinning. Visual field testing showed a 5-degree central scotoma in both eyes, and peripheral fields were limited to approximate 60 degrees in each eye.

By 2016, P1 had reported increasing flashing lights and more extreme photophobia. Visual acuity significantly decreased (20/160 right; 20/200 left). Binocular contrast sensitivity tested with a Pelli Robson chart was 0.75 (3/6 rows), indicating a significant loss of contrast sensitivity. Full-field electroretinography demonstrated a normal scotopic response, whereas photopic and flicker responses were markedly reduced, indicating a cone deficit. By 2022, visual acuity had further declined to 20/200 right and left. The previously noted mid-peripheral retinal sheen had intensified when examined clinically (Figure 1D). The sheen can be observed as a bright fundus surrounding the abnormal pigmentation in the macula (Figure 1D) and increased autofluorescence in the macula region (Figure 1E). Short-wavelength fundus autofluorescence revealed increased autofluorescence across the posterior pole, central hypoautofluorescence, and a central perifoveal ring of hyperautofluorescence (Figure 1E). A comparison of OCT imaging between 2013 and 2022 (Figure 1 C,F) suggested a 15% increase in ellipsoid zone dropout (2,840 µm versus 3253 µm). A detailed assessment of the outer retina (Figure 1C,F inserts) revealed an outer retina with normal thickness between the outer limiting membrane and the retinal pigment epithelium (~84 microns). For comparison, equivalent fundus (Figure 1G), autofluorescence (Figure 1H), and OCT images (Figure 1I) are provided from a normal subject. Notably, in patient OCT images, the normal stratification of signals was changed in that the stratification delineating the photoreceptor's outer segments was absent (cf. the Figure 1F insert with the normal retina 1I). In the presence of a normal thickness, we concluded that there was a change in the composition of the photoreceptor's outer segments rather than an atrophy of tissue.

Male subject 2 (P2) presented in 2021 at age 55 with a history of poor vision since his teenage years. A diagnosis of retinitis pigmentosa inversus (cone-rod dystrophy) had previously been made. P2 reported no useful central vision or reliance on peripheral vision for mobility. The subjects did not report night blindness, color vision deficiency, or issues with glare. His best-corrected visual acuity (BCVA)

was 20/400 right and 20/400 left. A dilated fundus examination revealed diffuse posterior pole atrophy involving the nasal and temporal retinas (Figure 2A). Short-wavelength fundus autofluorescence revealed posterior pole hyperautofluorescence increasing around the margin of central hypoautofluorescence (Figure 2B). OCT imaging revealed extensive outer retinal atrophy (Figure 2C).

The clinical phenotype in P2 is more severe than has been previously reported; however, the area of hyperautofluorescence surrounding the margin of central

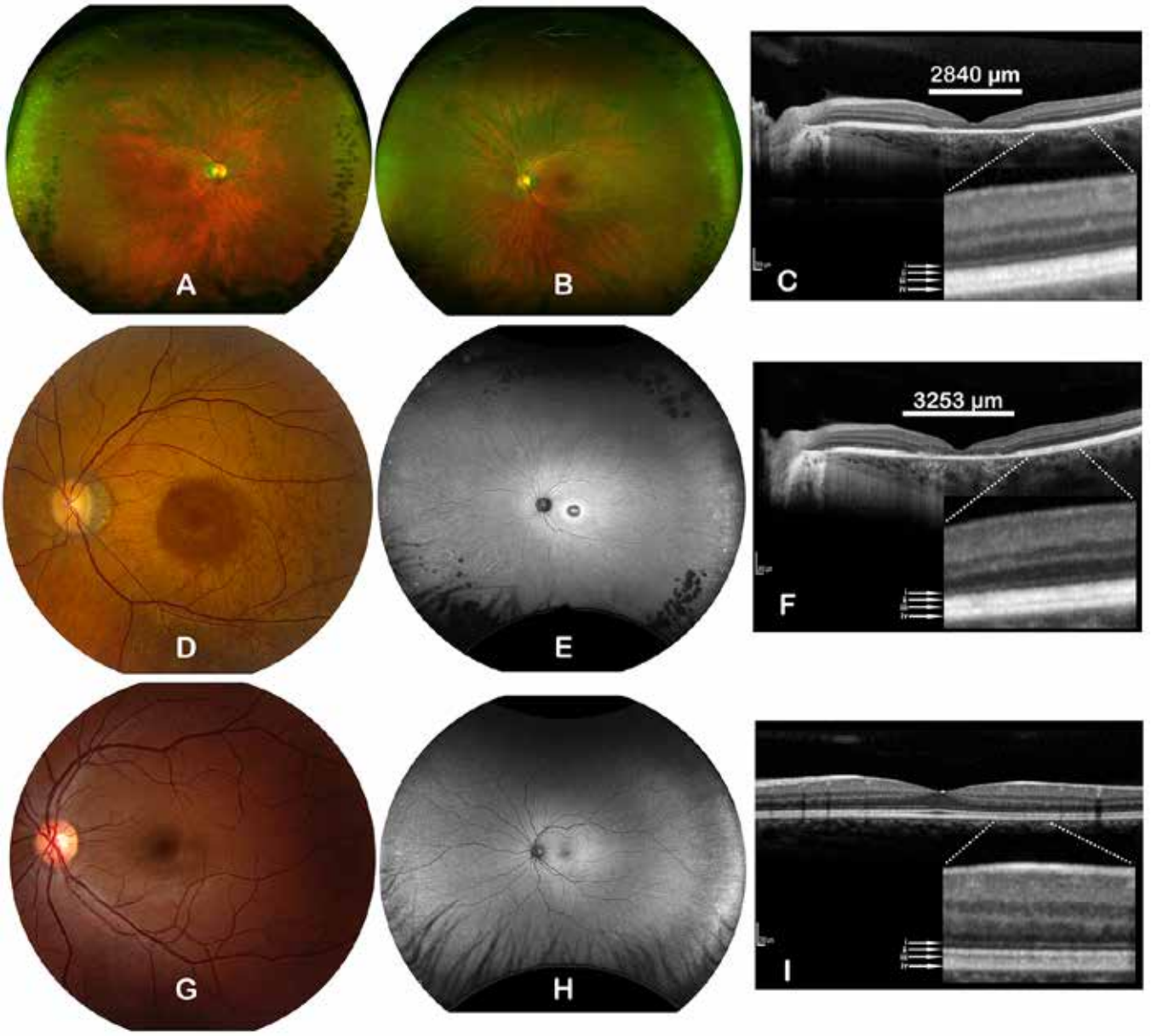

Figure 1. Retinal imaging for subject P1 (A–F) compared to a normal subject (G–I). (A, B) Wide-field retinal photography for P1 taken in 2013 shows pigmentary changes at both the macula plus Pearl degeneration in the peripheral retina. (**C**) SD–OCT imaging demonstrated an ellipsoid zone deficit (horizontal bar) in the left macula. (**D**) Repeat retinal photography in 2022 illustrated a dramatic retinal sheen associated with hyperautofluorescence (**E**) and further enlargement of the ellipsoid zone defect (**F**). Size bar=200 µm. Detailed assessment of the outer retina (**C**,**F** insert, dotted lines) revealed the normal thickness of the outer retina between the outer limiting membrane and the retinal pigment epithelium (~84 microns), but the absence of stratification delineating the photoreceptor's outer segments. Small white arrows indicate (i) the outer limiting membrane; (ii) the ellipsoid zone; (iii) the interdigitating zone; and (iv) Bruch's membrane/RPE complex. Representative images display the fundus (**G**), autofluorescence (H), and OCT imaging (**I**) from an unaffected individual.

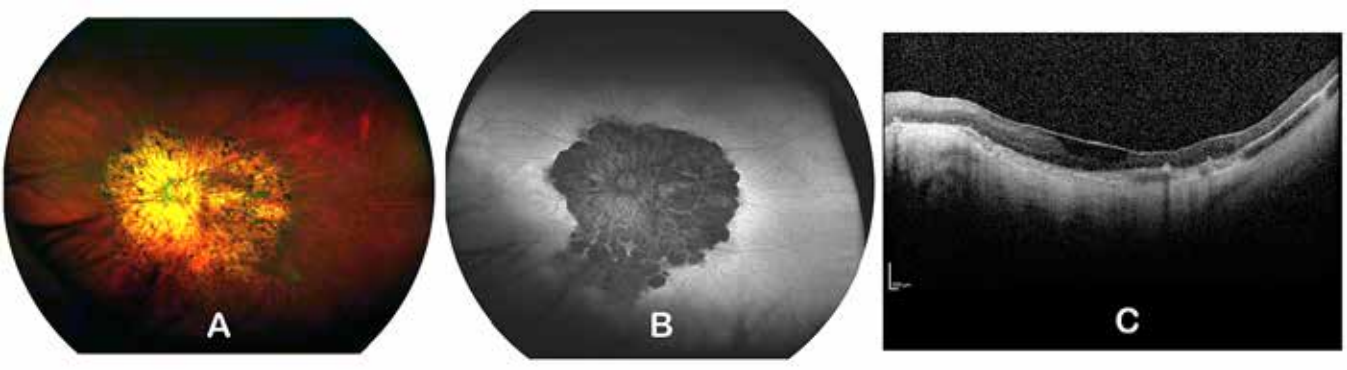

Figure 2. Retinal imaging for subject P2 (**A**–**C**). (**A**) Fundus imaging in P2 demonstrated widespread posterior pole chorioretinal atrophy surrounded by a rim of hyperautofluorescence (B). (**C**) SD–OCT imaging revealed widespread retinal atrophy (size bar=200 µm).

hyperautofluorescence at the posterior pole is a common finding. Patient P1 has a less severe phenotype than P2 but is in keeping with other reported *TTLL5* mutations [5,10,11].

Genetic testing results: Panel-based testing in P1 revealed a homozygous missense variant in the *TTLL5* gene c.1433G>A;p.(Arg478Gln). This missense variant has not been reported previously and was predicted to be deleterious by all in-silico prediction tools [POLYPHEN, SIFT, MUTTASTER]. Furthermore, the combined annotation dependent depletion (CADD) score at this nucleotide position is 29.3, which is very high (>20 considered highly conserved), placing this variant in the top 1% of deleterious variants in the human genome. Based on structural modeling using the missense3d package, we could make an unbiased prediction about the consequence of this missense mutation. The software predicts that the Arg478Gln substitution replaces a buried charged residue (Arg, RSA 6.4%) with an uncharged residue (Gln), which has a significant effect on the protein's structure. Thirteen individuals have been reported in gnomAD as heterozygous for this variant; however, no homozygous individuals have been reported. The affected amino acid is highly conserved in mammals and in evolutionarily more distant species, which suggests that this position does not tolerate variation (Figure 3A). This variant is in the c-terminal microtubule-binding domain of the protein that is required for interaction with the TTLL catalytic core domain [11]. The subject's son was examined and found asymptomatic with a normal eye exam.

In P2, panel-based testing identified two heterozygous variants in *TTLL5* that might be trans. The first variant c.2384_2387del;p.(Ala795Valfs*9) is absent from the gnomAD reference population. The affected amino acid is in the cofactor interaction domain (CID) of TTLL5, which interacts with $RPGR^{ORF15}$. The second variant identified was c.241C>G;p.(Leu81Val), which was also absent from the gnomAD reference population. This variant was predicted to be deleterious by all *in-silico* prediction tools. This missense variant is in the TTLL catalytic core domain of the protein that binds to ATP. The affected amino acids in each of these variants are highly conserved in mammals and other species (Figure 3B). No other variants were detected in this patient. The parents and siblings of P2 were negative for the phenotype, and his two children had a normal retinal exam. None of these family members was available for segregation analysis. By our *in-silico* analysis, the two missense variants we have identified (Arg478Gln; Leu81Val) are likely to be pathogenic; however, segregation analysis and functional studies are needed to confirm their pathogenicity. The location of these novel variants on the TTLL5 protein structure is shown in Figure 4.

DISCUSSION

Disease-causing mutations in *TTLL5* were initially reported with a CD phenotype, though this has now been extended to include CRD, sectoral CRD, and late-onset retinal dystrophy (Table 1). In this study, we report three novel *TTLL5* variants in two subjects with either CD or CRD. We identified a homozygous c.1433G>A;p.(Arg478Gln) variant in P1 with CD. This variant is in the c-terminal microtubule-binding domain of the protein. The only other reported variant in this domain is also a missense mutation (heterozygous c.1450C>T;p.Arg484Cys coupled with a frameshift mutation) causing sectoral CRD [11]. The phenotype for both mutations was diagnosed in the fourth decade of life, with progressive deterioration over time. Two other homozygous missense mutations have also been associated with CD but in other protein domains. The c.1627G>A;p.Glu543Lys mutation in the linker region of TTLL5 was associated with onset of CD symptoms at age 53 [5]. The other mutation c.2266A>T;p.Ile756Phe in the CID region of TTLL5 was

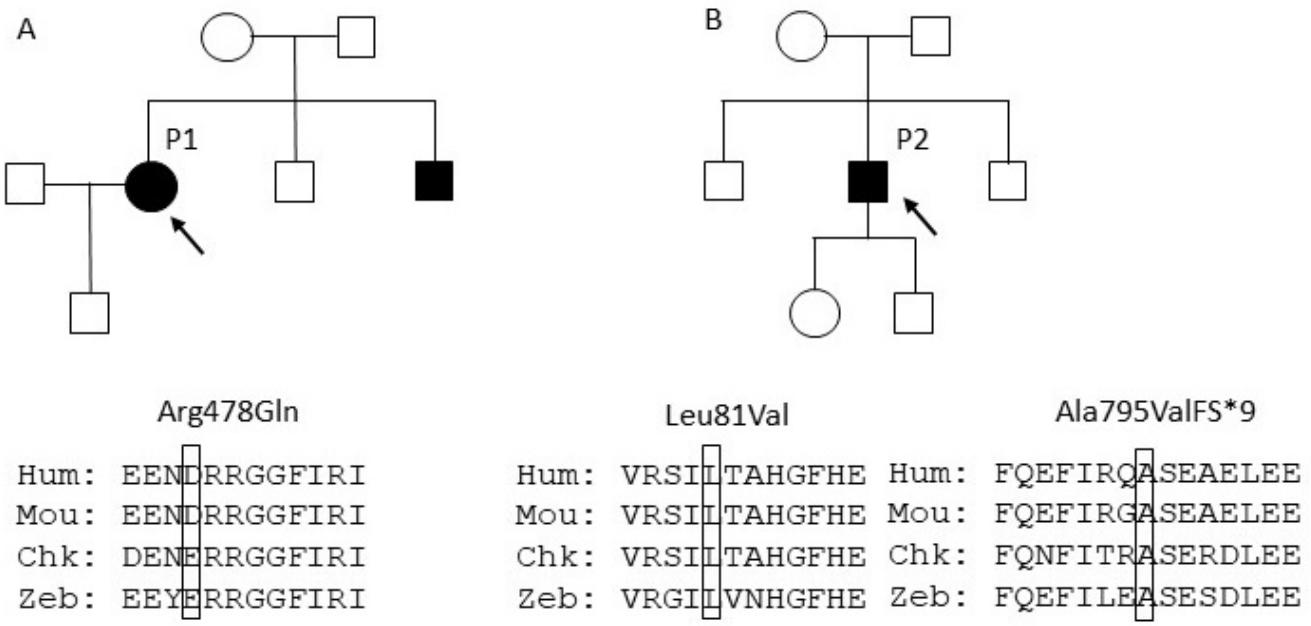

Figure 3. Evolutionary conservation of variant nucleotides identified by genetic testing. (**A**) Family tree for subject P1. The homozygous mutation affecting codon Arg478 is conserved in mouse (Mou), chicken (Chk), and zebrafish (Zeb) TTLL5 proteins. (**B**) Family tree for subject P2. The heterozygous mutation affecting codon Leu81 and the heterozygous mutation codon Ala795 are also conserved through evolution.

associated with the onset of CD at 38 years of age [6]. These observations suggest that missense mutations are associated with a later onset of the retinal phenotype. A homozygous missense mutation was reported to be associated with retinitis pigmentosa (c.1039T>C p.Phe347Leu in TTLL core domain). Nonetheless, there were no clinical data in the report to allow comparisons to be made [8].

In P2, we identified two heterozygous variants associated with early-onset CRD. The c.241C> G;p.Leu81Val variant is the first reported missense variant in the TTLL5 catalytic core domain. The other five reported mutations in the TTLL catalytic core domain are likely to result in truncated proteins derived from either in-frame nonsense mutations (two) causing CRD [6,10] or frameshifts that ultimately result in a nonsense mutation (three) causing CD [5,7,10]. All patients with a TTLL5 catalytic core domain mutation had an earlier onset of the retinal phenotype (range 9–28 years). The second variant we identified in P2 was c.2384_2387del;p.Ala795Valfs*9, which resides in the CID domain of TTLL5. This variant deletes 4 base pairs, generating a frameshift leading to a premature stop of codon 9 amino acids downstream. Although nonsense-mediated decay might be expected to degrade the transcript, a truncated protein could be produced. If such a truncated protein was produced, it would lack a catalytic core domain and would likely be non-functional. Two other loss-of-function mutations that affect the CID domain include a homozygous c.2132_2133insGATA;p.Met712Ilefs*15 mutation in a 58-year-old female patient diagnosed with CD [6] and a homozygous c.2029C>T;p.Arg677* mutation associated with CRD diagnosed in a female patient aged 46 [11]. Thus, mutations in the CID domain are not phenotype specific.

From the location of the variants in *TTLL5* identified in P1 and P2, we can infer the likely effect on protein function. The c.1433G>A;p.(Arg478Gln) variant in P1 is in the c-terminal microtubule binding domain of the protein. Hence, it is likely that microtubule binding is reduced because the loss of a positively charged arginine residue implies that TTLL5 can no longer interact with the negatively charged c-terminal of the α-tubulin, thereby interfering with protein transport [18]. Based on the two domain locations of the variants in P2, there is likely to be a significant effect on $RPGR^{ORF15}$ glutamylation, affecting the tracking of $RPGR^{ORF15}$ protein in the photoreceptor cilium. Cellular pulldown assays have demonstrated that the TTLL5 catalytic core domain interacts with the Glu–Gly repeat region of $RPGR^{ORF15}$ protein and the CID region interacts with the binding domain of $RPGR^{ORF15}$ [14]. In *Ttll5* knockout mouse, slow photoreceptor degeneration with early mislocalization of cone opsins is observed [14], mimicking the cone phenotype witnessed in patients.

Based on the observation that mice lacking *Ttll5* are infertile with defective sperm motility [19], it has been proposed that patients with mutations in *TTLL5* may have fertility problems [6]. Data from 6 families suggested that homozygous loss-of-function mutations in *TTLL5* were associated with reduced sperm motility and infertility, whereas missense mutations were not [6]. In other studies [5,10], fertility did not segregate with several loss-of-function mutations, including homozygous p.Glu543*; heterozygous p.Leu134Argfs*45;p.Trp1118*, and heterozygous p.Arg71*;p.Pro196Glufs*47 mutations. In our P2 subject, the heterozygous p.Ala795Valfs*9 variant is less likely to be associated with infertility, as he had 2 children. Correspondingly, growing evidence does not support the initial hypothesis that fertility directly relates to the TTLL5 genotype.

A notable observation in the *TTLL5*-associated retinal phenotype is the presence of a macular sheen best seen clinically, although the origin of this sheen has not been addressed in any studies reported thus far. In these studies, where OCT imaging was presented, ellipsoid dropout was a common finding, as were areas of hyperautofluorescence surrounding margins of central hypoautofluorescence in the perifoveal region of the retina [5,7,10,11]. In one study, increased hyperautofluorescence was noted over a 6-year period in one patient [6]. Interestingly, knockout mice for either the *Rpgr* or *Ttll5* genes show a change in their fundus color from orange to a metallic gray sheen [14]. Nevertheless, OCT imaging for these mice has not been performed. A macular sheen in humans has been observed in other phenotypes, including fenestrated sheen macular dystrophy [20], X-linked juvenile retinoschisis [21], female carriers of X-linked retinitis pigmentosa [22], and Muller cell sheen dystrophy [23]. Fenestrated sheen macular dystrophy is characterized by an irregular yellow lesion with red fenestrations [20]. Recently, autosomal recessive mutations in the *CRB1* gene have been identified in fenestrated sheen macular dystrophy [24]. Although there was a loss of the ellipsoid zone in the foveal region, the photoreceptor outer segment band was still present in the macula. In X-linked retinoschisis, an unusual sheen was associated with a mutation (p.Arg102Trp) in the *RS1* gene [19] before schisis cavities were present. The sheen seemed to be associated with major vascular arcades and was said to emanate from inner retinal

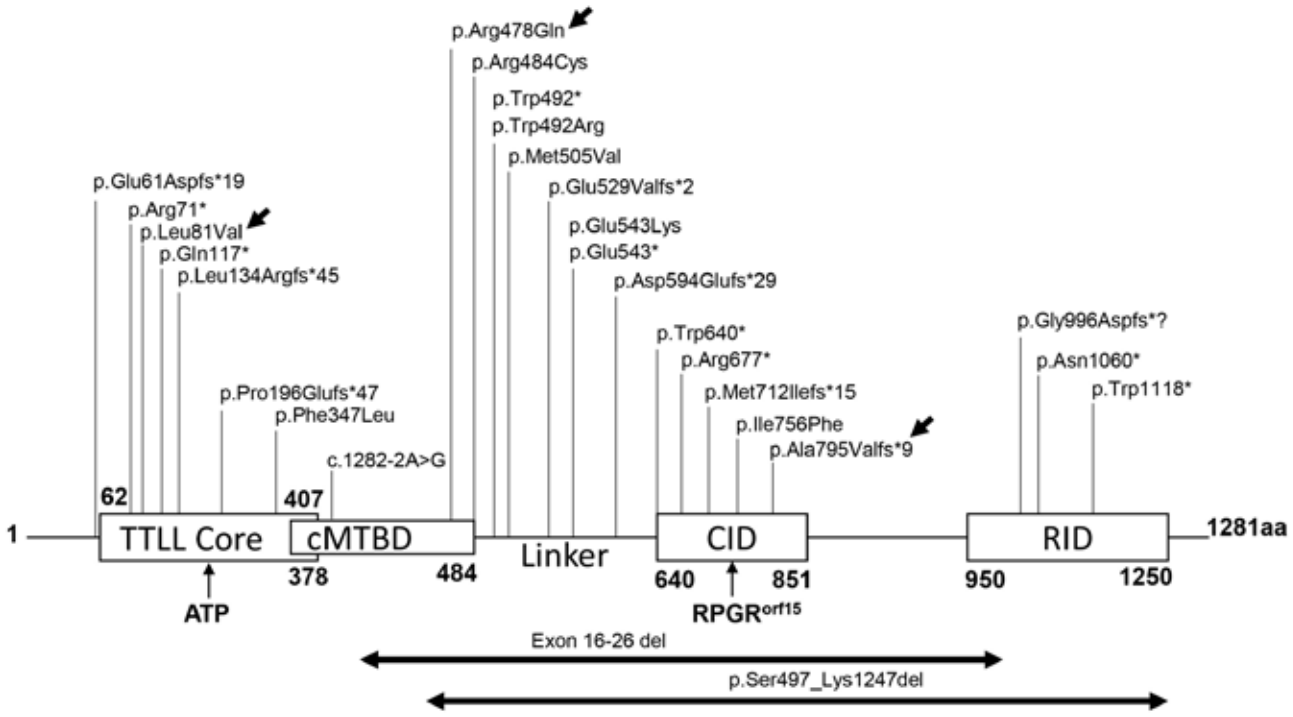

Figure 4. Topology of the TTLL5 protein and approximate location of all reported mutations. There are 4 major domains in the TTLL5 protein: the TTLL core domain that binds to ATP; an overlapping c-terminal microtubule binding domain (c-MTBD) that interacts with microtubulins; a linker region, followed by a cofactor interaction domain (CID) that interacts with to RPGR^{orf15}; and a receptor interaction domain (RID) of unknown function. Bold-type numbers identify the amino acid (aa) position relative to the location of each domain. Arrowhead: Mutations identified in this study. Double arrowhead lines represent previously reported large deletions in the TTLL5 protein.

Table 1. Mutations in *TTLL5* gene correlated to retinal phenotype.

Disease	Inheritance	cDNA	Protein	Protein domain	Variant type	Refs
CD	homozygous	c.182–3_182–1delinsAA	p.Glu61Aspfs*19	TTLL core	frameshift	Dias et al. 2017
CRD	compound heterozygous	c.211C>T c.585+2223_3326+ 5684del	p.Arg71* p.Pro196Glufs*47	TTLL core TTLL core/CID/RID	nonsense frameshift	Smirnov et al. 2021
CRD	compound heterozygous	c.241C>G c.2384_2387del	p.Leu81Val Ala795Valfs*9	TTLL core CID	missense frameshift	This paper
CRD	homozygous	c.349C>T	p.Gln117*	TTLL core	nonsense	Bedoni et al. 2016
CD	compound heterozygous	c.401del c.3354G>A	p.Leu134Argfs*45 Trp1118*	TTLL core RID	frameshift nonsense	Sergouniotis et al. 2014
RP	homozygous	c.1039T>C	p.Phe347Leu	TTLL core	missense	Patel et al. 2018
CD	homozygous	c.1433G>A	p.Arg478Gln	c-MTBD	missense	This paper
Sectoral CRD	compound heterozygous	c.1450C>T c.2987del	p.Arg484Cys p.Gly996Aspfs*?	c-MTBD RID	missense frameshift	Oh et al. 2022
CRD	compound heterozygous	c.1474T>A c.1627G>A	p.Trp492Arg p.Glu543Lys	Linker Linker	missense missense	Smirnov et al. 2021
CD + deafness	compound heterozygous	c.1475G>A c.3177_3180del	p.Trp492* p.Asn1060*	Linker RID	nonsense nonsense	Oh et al. 2022
CD	compound heterozygous	c.1487+1134_3741-2607delins15 c.1627G>A	p.Ser497_Lys1247del p.Glu543Lys	CID/RID Linker	frameshift missense	Smirnov et al. 2021
CD	compound heterozygous	c.1513A>G c.1282–2A>G	p.Met505Val p.?	Linker Linker	missense splicing mutation	Smirnov et al. 2021
CD	homozygous	c.1586_1589del	p.Glu529Valfs*2	Linker	frameshift	Sergouniotis et al. 2014
CRD	homozygous	c.1627G>T	p.Glu543*	Linker	nonsense	Sergouniotis et al. 2014
CD	homozygous	c.1627G>A	p.Glu543Lys	Linker	missense	Sergouniotis et al. 2014
CD	homozygous	c.1782del	p.Asp594Glufs*29	Linker	frameshift	Bedoni et al. 2016
EOSRD	homozygous	c.1920G>A	p.Trp640*	Linker	nonsense	Smirnov et al. 2021
CRD	homozygous	c.2029C>T	p.Arg677*	CID	nonsense	Oh et al. 2022
CD	homozygous	c.2132_2133insGATA	p.Met712Ilefs*15	CID	frameshift	Bedoni et al. 2016
CD	homozygous	c.2266A>T	p.Ile756Phe	CID	missense	Bedoni et al. 2016
CRD	homozygous	Exon 16–26 del	-	Linker/CID	large deletion	Mejecase et al. 2020

CD, cone dystrophy; CRD, cone-rod dystrophy; EOSRD, early-onset retinal dystrophy; RP, retinitis pigmentosa; TTLL core domain (amino acids 62 to 407) has a role in side chain elongation activity; c-MTBD (cationic microtubule binding domain - amino acids 378 to 488); Linker domain (amino acids 489–639); CID (cofactor interaction domain - amino acids 640 to 841); RID (receptor interaction domain) required for transcription factor function.

layers. Autosomal-dominant Muller cell sheen dystrophy is caused by a mutation in the transthyretin gene (p.Glu109Val) and has a cellophane-like appearance [25]. In this report, a longitudinal SD–OCT study revealed that the sheen was linked with increasing cystic changes in the inner retinal layers without initial macular involvement [25]. The retinal sheen observed with *TTLL5* mutations would appear distinct from other phenotypes in that OCT imaging suggests that this originates in photoreceptors' outer segments. Significantly, the edge of this retinal sheen changes with the increase in ellipsoid zone disruption with time in subject P1. It would also correlate with molecular studies suggesting that the focus of pathology in *TTLL5* mutations is the connecting cilium.

In conclusion, we report two subjects with 3 novel *TTLL5* variants exhibiting late-onset cone dystrophy and early-onset cone rod dystrophy. Vision loss and changes in retinal imaging in one subject show the progression of the disease over 9 years. Fundus photography correlated with SD-OCT imaging suggests that the macular sheen characteristically demonstrates with *TTLL5* mutations derives from the photoreceptor's outer segments at the posterior pole.

ACKNOWLEDGMENTS

This work was supported by a scholarship to OUK from the Experimental Medicine Graduate Program at UBC. We thank for Dr. A. Ebert for protein modeling analysis of the Arg478Gln mutation. CONFLICT OF INTEREST The authors state they have no conflicts of interest to declare

REFERENCES

1. Michaelides M, Hardcastle AJ, Hunt DM, Moore AT. Progressive cone and cone-rod dystrophies: phenotypes and underlying molecular genetic basis. Surv Ophthalmol 2006; 51:232-58. [PMID: 16644365].

2. Birtel J, Eisenberger T, Gliem M, Müller PL, Herrmann P, Betz C, Zahnleiter D, Neuhaus C, Lenzner S, Holz FG, Mangold E, Bolz HJ, Charbel Issa P. Clinical and genetic characteristics of 251 consecutive patients with macular and cone/cone-rod dystrophy. Sci Rep 2018; 8:4824-[PMID: 29555955].

3. Roosing S, Thiadens AA, Hoyng CB, Klaver CC, den Hollander AI, Cremers FP. Causes and consequences of inherited cone disorders. Prog Retin Eye Res 2014; 42:1-26. [PMID: 24857951].

4. Nagase T, Ishikawa K, Suyama M, Kikuno R, Hirosawa M, Miyajima N, Tanaka A, Kotani H, Nomura N, Ohara O. Prediction of the coding sequences of unidentified human genes. XIII. The complete sequences of 100 new cDNA clones from brain which code for large proteins in vitro. DNA Res 1999; 6:63-70. [PMID: 10231032].

5. Sergouniotis PI, Chakarova C, Murphy C, Becker M, Lenassi E, Arno G, Lek M, MacArthur DG, Bhattacharya SS, Moore AT, Holder GE, Robson AG, Wolfrum U, Webster AR, Plagnol V. UCL-Exomes Consortium. Biallelic variants in TTLL5, encoding a tubulin glutamylase, cause retinal dystrophy. Am J Hum Genet 2014; 94:760-9. [PMID: 24791901].

6. Bedoni N, Haer-Wigman L, Vaclavik V, Tran VH, Farinelli P, Balzano S, Royer-Bertrand B, El-Asrag ME, Bonny O, Ikonomidis C, Litzistorf Y, Nikopoulos K, Yioti GG, Stefaniotou MI, McKibbin M, Booth AP, Ellingford JM, Black GC, Toomes C, Inglehearn CF, Hoyng CB, Bax N, Klaver CC, Thiadens AA, Murisier F, Schorderet DF, Ali M, Cremers FP, Andréasson S, Munier FL, Rivolta C. Mutations in the polyglutamylase gene *TTLL5*, expressed in photoreceptor cells and spermatozoa, are associated with cone-rod degeneration and reduced male fertility. Hum Mol Genet 2016; 25:4546-55. [PMID: 28173158].

7. . Dias MdS. Hamel CP, Meunier I, Varin J, Blanchard S, Boyard F, Sahel J-A, Zeitz C. Novel splice-site mutation in TTLL5 causes cone dystrophy in a consanguineous family. Mol Vis 2017; 23:131-9. .

8. Patel N, Alkuraya H, Alzahrani SS, Nowailaty SR, Seidahmed MZ, Alhemidan A, Ben-Omran T, Ghazi NG, Al-Aqeel A, Al-Owain M, Alzaidan HI, Faqeih E, Kurdi W, Rahbeeni Z, Ibrahim N, Abdulwahab F, Hashem M, Shaheen R, Abouelhoda M, Monies D, Khan AO, Aldahmesh MA, Alkuraya FS. Mutations in known disease genes account for the majority of autosomal recessive retinal dystrophies. Clin Genet 2018; 94:554-63. [PMID: 30054919].

9. Méjécase C, Kozak I, Moosajee M. The genetic landscape of inherited eye disorders in 74 consecutive families from the United Arab Emirates. Am J Med Genet C Semin Med Genet 2020; 184:762-72. [PMID: 32783370].

10. Smirnov V, Grunewald O, Muller J, Zeitz C, Obermaier CD, Devos A, Pelletier V, Bocquet B, Andrieu C, Bacquet JL, Lebredonchel E, Mohand-Saïd S, Defoort-Dhellemmes S, Sahel JA, Dollfus H, Zanlonghi X, Audo I, Meunier I, Boulanger-Scemama E, Dhaenens CM. Novel TTLL5 variants associated with cone-rod dystrophy and early-onset severe retinal dystrophy. Int J Mol Sci 2021; 22:6410-[PMID: 34203883].

11. Oh JK, Vargas Del Valle JG, Lima de Carvalho JR Jr, Sun YJ, Levi SR, Ryu J, Yang J, Nagasaki T, Emanuelli A, Rasool N, Allikmets R, Sparrow JR, Izquierdo NJ, Duncan JL, Mahajan VB, Tsang SH. Expanding the phenotype of TTLL5-associated retinal dystrophy: a case series. Orphanet J Rare Dis 2022; 17:146-[PMID: 35365235].

12. Ikegami K, Sato S, Nakamura K, Ostrowski LE, Setou M. Tubulin polyglutamylation is essential for airway ciliary function through the regulation of beating asymmetry. Proc Natl Acad Sci U S A 2010; 107:10490-5. [PMID: 20498047].

13. Hong D-H, Pawlyk B, Sokolov M, Strissel KJ, Yang J, Tulloch B, Wright AF, Arshavsky VY, Li T. RPGR isoforms in photoreceptor connecting cilia and the transitional zone of motile

cilia. Invest Ophthalmol Vis Sci 2003; 44:2413-21. [PMID: 12766038].

14. Sun X, Park JH, Gumerson J, Wu Z, Swaroop A, Qian H, Roll-Mecak A, Li T. Loss of RPGR glutamylation underlies the pathogenic mechanism of retinal dystrophy caused by TTLL5 mutations. Proc Natl Acad Sci U S A 2016; 113:E2925-34. [PMID: 27162334].

15. Richards S, Aziz N, Bale S, Bick D, Das S, Gastier-Foster J, Grody WW, Hegde M, Lyon E, Spector E, Voelkerding K, Rehm HL. ACMG Laboratory Quality Assurance Committee. Standards and guidelines for the interpretation of sequence variants: a joint consensus recommendation of the American College of Medical Genetics and Genomics and the Association for Molecular Pathology. Genet Med 2015; 17:405-24. [PMID: 25741868].

16. Ittisoponpisan S, Islam SA, Khanna T, Alhuzimi E, David A, Sternberg MJE. Can predicted protein 3D structures provide reliable insights into whether missense variants are disease associated? J Mol Biol 2019; 431:2197-212. [PMID: 30995449].

17. Jumper J, Evans R, Pritzel A, Green T, Figurnov M, Ronneberger O, Tunyasuvunakool K, Bates R, Žídek A, Potapenko A, Bridgland A, Meyer C, Kohl SAA, Ballard AJ, Cowie A, Romera-Paredes B, Nikolov S, Jain R, Adler J, Back T, Petersen S, Reiman D, Clancy E, Zielinski M, Steinegger M, Pacholska M, Berghammer T, Bodenstein S, Silver D, Vinyals O, Senior AW, Kavukcuoglu K, Kohli P, Hassabis D. Highly accurate protein structure prediction with AlphaFold. Nature 2021; 596:583-9. [PMID: 34265844].

18. Hausrat TJ, Janiesch PC, Breiden P, Lutz D, Hoffmeister-Ullerich S, Hermans-Borgmeyer I, Failla AV, Kneussel M. Disruption of tubulin-alpha4a polyglutamylation prevents aggregation of hyper-phosphorylated tau and microglia activation in mice. Nat Commun 2022; 13:4192-[PMID: 35858909].

19. Lee GS, He Y, Dougherty EJ, Jimenez-Movilla M, Avella M, Grullon S, Sharlin DS, Guo C, Blackford JA Jr, Awasthi S, Zhang Z, Armstrong SP, London EC, Chen W, Dean J, Simons SS Jr. Disruption of Ttll5/stamp gene (tubulin tyrosine ligase-like protein 5/SRC-1 and TIF2-associated modulatory protein gene) in male mice causes sperm malformation and infertility. J Biol Chem 2013; 288:15167-80. [PMID: 23558686].

20. O'Donnell FE Jr, Welch RB. Fenestrated sheen macular dystrophy. A new autosomal dominant maculopathy. Arch Ophthalmol 1979; 97:1292-6. [PMID: 454265].

21. Robson AG, Mengher LS, Tan MH, Moore AT. An unusual fundus phenotype of inner retinal sheen in X-linked retinoschisis. Eye (Lond) 2009; 23:1876-8. [PMID: 19741719].

22. Kilgore DA, Kilgore TA, Sukpraprut-Braaten S, Schaefer GB, Uwaydat SH. Multimodal imaging of an RPGR carrier female. Ophthalmic Genet 2021; 42:312-6. [PMID: 33620278].

23. Parida H, Kannan NB, Rathinam SR. Imaging of Muller cell sheen dystrophy. Indian J Ophthalmol 2020; 68:533-5. [PMID: 32057027].

24. Oh DJ, Daily MJ, Grassi MA. CRB1 maculopathy presenting as fenestrated sheen macular dystrophy with 15-year follow-up. Doc Ophthalmol 2021; 142:381-8. [PMID: 33387055].

25. Dalma-Weiszhausz J, Chacón-Camacho O, Chevez-Barrios P, Zenteno JC, Franco-Cárdenas V, García-Montaño LA, Pérez-Bravo J, García-Montalvo IA, Jiménez-Sierra JM, Dalma A. Autosomal dominant Muller cell sheen dystrophy: clinical, histopathologic, and genentic assessment in an extended family with long follow-up. Retina 2022; 42:981-91. [PMID: 35125479].

Articles are provided courtesy of Emory University and the Zhongshan Ophthalmic Center, Sun Yat-sen University, P.R. China. The print version of this article was created on 15 December 2023. This reflects all typographical corrections and errata to the article through that date. Details of any changes may be found in the online version of the article.